Rigid unit modes and intrinsic flexibility in linearly bridged framework structures

Andrew L. Goodwin
Department of Earth Sciences, Cambridge University, Downing Street, Cambridge CB2 3EQ, United Kingdom
(Received 15 June 2006; published 13 October 2006)

A method of calculating the number and nature of rigid unit modes (RUMs) in linearly bridged framework structures is presented. Using this approach, it is shown that linearly bridged framework structures inherently possess large degrees of structural flexibility, irrespective of their connectivity (i.e., framework topology). In particular, an $O(V)$ density of RUMs across reciprocal space is an intrinsic property of these materials. This result has implications for their guest sorption, ion diffusion, strain screening, and negative thermal expansion behavior. The RUM spectra of three representative topologies are studied: the Prussian Blue, $Zn(CN)_2$, and extended β-quartz structure types.

DOI: 10.1103/PhysRevB.74.134302 PACS number(s): 63.20.−e, 61.50.Ah, 65.40.De

I. INTRODUCTION

Many framework materials (e.g., perovskites, silicates, zeolites) are composed of corner- or edge-sharing metal coordination polyhedra, connected to form a large variety of three-dimensional topological nets (see, for example, Ref. 1). The observation that phase transitions in these materials often involve relative rotations and translations of the "rigid" metal coordination units (polyhedra) of which they are composed[2–6] has led to the development of systematic methods of calculating the rigid unit modes (RUMs) in these (and related) compounds.[7] RUMs are those phonon modes that can propagate throughout the crystal lattice while preserving bond lengths and metal coordination geometries. They involve translations and/or rotations of the coordination polyhedra; the only form of local deformation that occurs is flexing at the connections between polyhedra. These modes form a subset of the complete dynamical spectrum and tend to occur at low frequencies, by virtue of the energetically inexpensive local deformations involved. Moreover, they often exhibit strongly pressure- and/or temperature-dependent behavior; this is responsible for their predominant role in soft-mode (displacive) phase transitions.

The use of the RUM model to simplify lattice dynamics in framework materials has gained currency through its ability to explain a variety of physical phenomena; perhaps the highest profile of these is negative thermal expansion (NTE) behavior.[8,9] The vast majority of compounds known to exhibit NTE at ambient conditions have open framework structures that support RUMs.[9–11] While the RUMs constitute only a part of their low-energy phonon spectrum, their reciprocal space density and the large and negative Grüneisen parameters with which they are associated in these materials are sufficient to dominate their bulk thermal expansion behavior. A well-studied example is that of ZrW_2O_8, which possesses RUMs and quasi-RUMs (QRUMs; modes that involve only very small deformations of rigid units) at all points in reciprocal space;[8] this ensures a thermodynamic density of (Q)RUMs in the phonon spectrum. The population of (Q)RUMs in this material has been verified experimentally, and shows evidence for contributions from the entire ensemble of modes.[12]

But RUMs explain more than the existence of phase transitions and NTE behavior: they reflect the extent of inherent framework flexibility and its role in a variety of other physical phenomena. Structural rigidity has emerged as an area of vital importance for the study of crystals,[13,14] glasses,[15–17] and indeed macromolecular assemblies such as proteins.[18] In the context of RUMs in crystalline materials, one example of unusual behavior is the ability of zeolites to adsorb a range of species on the surface of their internal cavities.[19] The local stress associated with the adsorption process can be dissipated almost entirely through rotations and translations of rigid units in the surrounding region. The zeolite frameworks are able to accommodate stress in this way only because their structures possess a very large number $[O(V)]$ of RUMs across reciprocal space, and so local deformations are possible through the linear superposition of many modes.[19] These RUM "wave-packets" also allow zeolite-guest complexes to attain specific geometries required for catalytic behavior with virtually no associated cost in elastic energy.[20] Similar local deformations provide a mechanism for ion conduction in, e.g., β-eucryptite (Ref. 21) and strain screening in cation-substituted ("stuffed") framework structures.[22]

There is strong interest in the identification of compounds whose structures possess large numbers of RUMs. On the one hand, the large associated spectral weight means that unusual thermodynamic properties of the modes (e.g., negative Grüneisen parameters) are more likely to dominate the bulk behavior. On the other hand, the existence of RUMs at an arbitrary wave vector signals the existence of localized flexible regions—individual polyhedra or groups of polyhedra that can flex without disturbing the surrounding structural environment—responsible for atypical sorption and catalytic properties. Consequently RUM-dense materials might be expected to exhibit an array of interesting physical properties. In this respect, it is interesting that one can increase flexibility in a given framework geometry by introducing rigid "rods" between connected polyhedra (Fig. 1). It was Simon and Varma that first set about quantifying this increase in flexibility (albeit using a slightly different language to that of RUMs): they studied the incorporation of linear bridging units (more precisely, light inextensible rods) into a simple two-dimensional perovskite topology and its effect on various thermodynamic properties.[23] What they found was that the single nontrivial RUM of the original topology (at $\mathbf{k}=\langle\frac{1}{2}\frac{1}{2}\rangle^*$) exploded into a dense family of

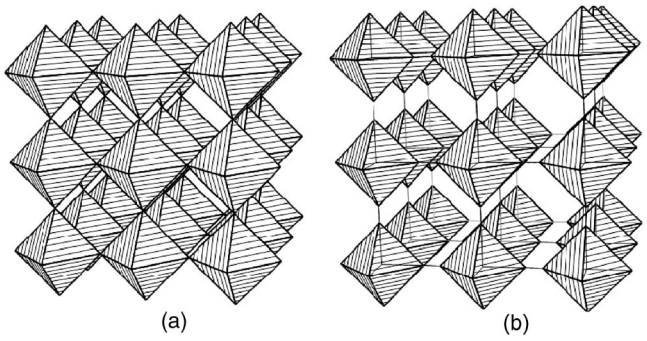

FIG. 1. Polyhedral representations of the (a) perovskite and (b) idealized Prussian Blue lattices. The two topologies share the same arrangement of polyhedra, but pairs of adjacent polyhedra are spaced relative to each other in (b) by the incorporation of rodlike linkages.

RUMs at all wave vectors with this seemingly trivial change in geometry. The RUMs were sufficiently many to decouple the rotational degrees of freedom of the "rigid units."

Framework materials that possess these linearly bridged topologies are well-known: perhaps the best characterized examples are the Prussian Blue analogs, whose structures consist of metal centers linked by linear cyanide (CN^-) ions, which by virtue of the very strong C-N bond act as essentially inextensible rods.[24–27] In fact, many members of the broad and diverse family of cyanide-bridged framework materials share this same basic motif.[25,26] It is of interest then that NTE behavior has been reported in increasingly many of these compounds.[28–34] For some of these, the number of RUMs across the Brillouin zone (BZ) has been determined; as for the two-dimensional Simon and Varma example, each such structure appears to possess RUMs at all points in reciprocal space.[30] Moreover, these modes are all associated with negative Grüneisen parameters: it is likely that many—if not all—of the RUMs contribute in some way to the NTE behavior. Other linearly bridged framework materials are notable for their sorption properties[35] and "molecular magnetism."[27]

If one is to understand the physical manifestation of RUMs in these systems, a robust method of calculating their density and associated atomic displacements is essential. The existing methods for calculating RUMs in framework systems with single-atom bridges (i.e., those that consist of corner- or edge-sharing polyhedra, referred to hereafter as "classical" framework systems) can be modified to calculate RUMs in linearly bridged systems;[7] these methods are discussed in more detail below. Indeed it is by using modifications of this sort that the RUMs in some linearly bridged topologies have already been quantified.[30,36] It would also be possible to approach these calculations analytically, developing the relevant theory on a case-by-case basis, in a manner similar to that of Simon and Varma.[23] However, the key focus of this paper is the development of an approach specific to linearly bridged frameworks, with the particular advantage that it allows some general conclusions to be drawn concerning flexibility in these systems. The methodology is developed from the split-atom dynamical matrix approach already employed to study RUMs in "classical" framework systems.

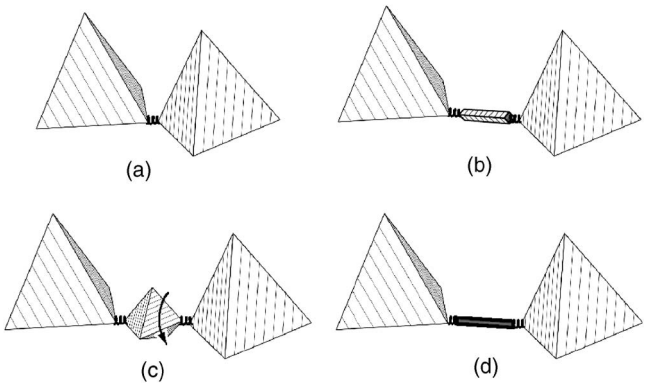

FIG. 2. (a) A representation of the split-atom interactions used in the CRUSH dynamical matrix approach for calculating RUMs. Connected vertices of adjacent polyhedra are joined by a fictitious spring of zero equilibrium length. (b) Linear linkages modeled as rodlike polyhedra in CRUSH with five degrees of freedom. (c) Linear linkages modeled as underconstrained polyhedra in CRUSH. The CRUSH output will contain contributions from additional, unphysical modes that correspond to rotation of these polyhedra about their constrained axes. (d) The "constant separation" approach redefines the interaction potential used to build the dynamical matrix so that connected vertices of adjacent polyhedra are considered to be joined by a spring of nonzero equilibrium length (represented here as the solid portion of the spring).

The theoretical framework that underpins the approach is described in Sec. II, together with its implementation in the computer program LUSH. The approach is applied to three structure types in Sec. III: the Prussian Blue, $Zn(CN)_2$, and $Zn[M(CN)_2]_2$ families. The discussion presented in Sec. IV centers on the general results implicit in the theory of Sec. II. In particular, it is shown that large RUM densities are ubiquitous among linearly bridged framework topologies: the remarkable decoupling of degrees of freedom found by Simon and Varma is shown to generalize to arbitrary framework topologies.

II. THEORY

A. Background: The split-atom approach

For "classical" frameworks, the split-atom approach is the method of choice for calculating the number and nature of RUMs across reciprocal space.[7] This is a molecular dynamical matrix approach that treats each coordination polyhedron j as an individual molecule with six degrees of freedom: three translational (u_{jx}, u_{jy}, u_{jz}) and three rotational $(\theta_{jx}, \theta_{jy}, \theta_{jz})$. The particular framework topology in question dictates the pairs of polyhedral vertices that are considered "connected." A fictitious spring of zero equilibrium length is then constructed between each vertex in these pairs [Fig. 2(a)]. The Hamiltonian is built from the harmonic interaction parameters $\varphi_{jj'}$, which in turn depend on the length $d_{jj'}$ of each "spring:"

$$\varphi_{jj'} = \frac{1}{2} K d_{jj'}^2. \tag{1}$$

The force constant $K > 0$ is the only adjustable parameter in the model and can be varied so as to give physically sensible

phonon frequencies. A dynamical matrix is constructed from the φ and is analyzed in the usual way. The RUMs appear as the set of eigenvectors of the dynamical matrix whose associated eigenvalue is identically zero (i.e., they form a basis for the kernel of the dynamical matrix); consequently their nature does not depend on the particular value of K chosen.

While the split-atom dynamical model is based upon the concept of shared atoms being "split" between pairs of polyhedra, the model itself is not as unphysical as perhaps it first appears. To a first approximation, the force constant K represents the energy penalty associated with deformations of the polyhedra, and one finds at least qualitative similarity between the calculated phonon dispersion and that observed experimentally.[7] It is of course a very simplistic view of the important interactions in a framework material; however, additional complexity is not necessary to identify the RUMs. A more elaborate approach would be needed to discriminate further from among the RUMs those that are likely to occur at lowest energy. The split-atom method necessarily assigns all RUMs as zero-frequency modes: the small energy penalty involved in flexing at polyhedral connections is ignored. In practice, different RUMs will involve different forms of interpolyhedral flexing, and so will occur at different frequencies.

There are two possible ways of using the split-atom approach to identify RUMs in linearly bridged framework systems. First, the linear linkages can be modeled as polyhedra with five degrees of freedom: three translational and two rotational (rotations about the "rod" axis being considered unphysical) [Fig. 2(b)]. Second, the linkages can be modeled as ordinary polyhedra (i.e., with six degrees of freedom), but with unconstrained vertices [Fig. 2(c)].[30,36] The latter method introduces a number of spurious RUMs that must be discounted: these correspond to rotations of the artificial polyhedra about the corresponding rod axis. Correctly interpreted, both approaches do of course identify the same RUM spectrum, and these methods have been employed elsewhere in a handful of cases to investigate RUMs in simple cyanide topologies.[30,36]

B. The constant separation approach

The approach developed in this study differs from these two applications of the split-atom method in that it does not treat the linear bridges as polyhedra in their own right, but as constraints on the coordination polyhedra they connect. As such the approach is applicable specifically to linearly bridged systems. Because of this specificity, it will be shown that a number of general results can be derived concerning flexibility in these important framework materials. Moreover, the approach lends itself readily to symmetry analysis.

The basic idea is that linear bridges act to constrain the distance between the polyhedral vertices they connect. This interpretation suggests a method of extending the split-atom approach to simplify the calculation of RUMs in these systems: the key concept is to consider the springs to have a nonzero equilibrium length that corresponds to the length of the bridging rods themselves [Fig. 2(d)]. That is, Eq. (1) is replaced by

$$\varphi_{jj'} = \frac{1}{2}K(d_{jj'} - \bar{d}_{jj'})^2, \tag{2}$$

where $\bar{d}_{jj'} > 0$ is the equilibrium length of the relevant bridging rod. The connected atoms are now no longer "split," but connected by an extensible rod, whose extension is associated with an energy penalty. The RUMs implicit in Eq. (1) are those modes that maintain a distance of *zero* between connected polyhedral vertices; Eq. (2) now defines RUMs as modes that maintain a distance of $\bar{d}_{jj'}$ between vertices. That is, the kernel of the new dynamical matrix will contain only those sets of polyhedral translations and rotations that preserve the *separation* between connected vertices. These correspond to linear superpositions of the RUMs of the linearly bridged framework.

To establish the form of the dynamical matrix constructed using this "constant separation" approach, the effect of small displacements $\mathbf{u}_j = [u_{jx}\ u_{jy}\ u_{jz}]^{\mathrm{T}}$ and small rotations

$$\mathbf{R}_j = \begin{bmatrix} 1 & -\theta_{jz} & \theta_{jy} \\ \theta_{jz} & 1 & -\theta_{jx} \\ -\theta_{jy} & \theta_{jx} & 1 \end{bmatrix}$$

on the separation $d_{jj'}$ between connected vertices is considered. Each vertex is characterized by a vector $\mathbf{e}_j$ drawn from the polyhedral center of mass to the vertex itself. Then the translations and rotations map $\mathbf{e}_j$ to $\mathbf{u}_j + \mathbf{R}_j \cdot \mathbf{e}_j$ and $\mathbf{e}_{j'}$ to $\mathbf{u}_{j'} + \mathbf{R}_{j'} \cdot \mathbf{e}_{j'}$. The separation between the two vertices is similarly mapped from $\bar{\mathbf{d}}_{jj'}$ to a new vector

$$\mathbf{d}_{jj'} = \bar{\mathbf{d}}_{jj'} + (\mathbf{e}_j - \mathbf{R}_j \cdot \mathbf{e}_j - \mathbf{u}_j) - (\mathbf{e}_{j'} - \mathbf{R}_{j'} \cdot \mathbf{e}_{j'} - \mathbf{u}_{j'}).$$

It can be shown that the deviation $\Delta d = d_{jj'} - \bar{d}_{jj'} = |\mathbf{d}_{jj'}| - |\bar{\mathbf{d}}_{jj'}|$ is given by

$$\Delta d = \boldsymbol{\rho} \cdot [(\mathbf{e}_j - \mathbf{R}_j \cdot \mathbf{e}_j - \mathbf{u}_j) - (\mathbf{e}_{j'} - \mathbf{R}_{j'} \cdot \mathbf{e}_{j'} - \mathbf{u}_{j'})], \tag{3}$$

where $\boldsymbol{\rho}$ is a unit vector in the direction of $\bar{\mathbf{d}}_{jj'}$. The absolute length of the interpolyhedral rods does not enter Eq. (3): the dynamical matrix depends only on their orientation.

The force-constant matrix $\boldsymbol{\phi}$ from which the dynamical matrix is constructed has elements

$$\phi_{gh} = K\frac{\partial(\Delta d)}{\partial g_j}\frac{\partial(\Delta d)}{\partial h_{j'}}; \quad g,h \in \{u_x,u_y,u_z,\theta_x,\theta_y,\theta_z\},$$

and so the dynamical matrix[37] is built from 6×6 blocks of the form

$$K\left[\begin{array}{c|c} \mathrm{A} & \mathrm{B} \\ \hline \mathrm{C} & \mathrm{D} \end{array}\right]\exp[i\mathbf{k}\cdot(\mathbf{r}_{j'} - \mathbf{r}_j)], \tag{4}$$

where

$$A_{\alpha\beta} = -\rho_\alpha\rho_\beta,$$

$$B_{\alpha\beta} = \rho_\alpha(\rho_{\beta'}e_{j'\beta''} - \rho_{\beta''}e_{j'\beta'}),$$

$$C_{\alpha\beta} = \rho_\beta(\rho_{\alpha'}e_{j\alpha''} - \rho_{\alpha''}e_{j\alpha'}),$$

$$D_{\alpha\beta} = -(\rho_{\alpha'} e_{j\alpha''} - \rho_{\alpha''} e_{j\alpha'})(\rho_{\beta'} e_{j'\beta''} - \rho_{\beta''} e_{j'\beta'}),$$

$\alpha, \beta \in \{x,y,z\}$ and $\alpha = x \Rightarrow \alpha' = y, \alpha'' = z$, etc. Each such block corresponds to a single linear bridge in the framework unit cell. The dynamical matrix is assembled in the usual manner, and the RUMs of the linearly bridged framework identified as those eigenvectors of the dynamical matrix with eigenvalues equal to zero.

C. Symmetry considerations

With a knowledge of the symmetry of the framework structure in question, group theoretical analysis can be used to simplify the form of the dynamical matrix. Group theory also allows the eigenvectors of the dynamical matrix to be classified according to their symmetry, and so RUMs of different symmetry can be separated automatically. Because the constant separation approach uses a polyhedral representation of the framework structure itself (i.e., does not involve any additional, "imaginary" atoms or polyhedra), a group-theoretical analysis of the native framework can be used directly in the dynamical matrix calculations. [The approach illustrated in Fig. 2(c) would generally preclude the use of group theory in this way.]

The studies of normal modes in crystals by Maradudin and Vosko[38] and by Warren[39] illustrate how one might arrive at a set of symmetry coordinates $\mathbf{e}_i(\mathbf{k})$ that describe a basis in which the dynamical matrix $\mathbf{D}(\mathbf{k})$ is in block-diagonal form. Assembling the $\mathbf{e}_i(\mathbf{k})$ into the unitary matrix $\mathbf{S}(\mathbf{k})$, one has

$$\mathbf{S}^{-1}(\mathbf{k}) \cdot \mathbf{D}(\mathbf{k}) \cdot \mathbf{S}(\mathbf{k}) = \mathbf{D}_{\mathrm{SR}}(\mathbf{k}),$$

where "SR" signifies "symmetry reduced" and $\mathbf{S}^{-1}(\mathbf{k}) = \mathbf{S}^{\mathrm{T}}(-\mathbf{k})$. The $\mathbf{e}_i(\mathbf{k})$ are eigenvectors of $\mathbf{D}_{\mathrm{SR}}(\mathbf{k})$, such that each one can be associated with a single irreducible representation of the point group of the wave vector. Each block in $\mathbf{D}_{\mathrm{SR}}(\mathbf{k})$ corresponds to one and only one of these irreducible representations, and so modes of different symmetries are precluded from mixing.

D. Implementation

A computational implementation of the constant separation approach follows naturally from the existing program CRUSH, written by Giddy *et al.* to calculate RUMs in "classical" framework systems.[7] The program CRUSH is itself a modification of the earlier molecular dynamics program CRASH, written by Pawley.[40] The newly modified version, called LUSH (Linear crUSH), was programmed essentially identically, except for the following alterations.

1. The number and connectivity of linear linkages are inferred from the positions of the framework polyhedra: pairs of vertices separated by some predetermined distance (say, within 0.05 Å of 1.0 Å) are assumed to be connected by a linear rod. The rod orientation (i.e., the appropriate value of $\boldsymbol{\rho}$) is determined by normalization of the vector drawn from one vertex to its connected pair.

2. The dynamical matrix is calculated using the formalism of Eq. (4).

3. The program is interfaced internally with the group-theoretical program GROUP2 of Warren and Worlton so that the implicit symmetry constraints on the dynamical matrix are automatically taken into account wherever possible.[39,41,42]

The program calculates the normal mode frequencies via diagonalization of the blocks in $\mathbf{D}_{\mathrm{SR}}(\mathbf{k})$. The eigenvalues give the squared normal mode frequencies, and the eigenvectors describe the rigid unit displacement/rotation patterns associated with each mode.

III. CASE STUDIES

This section describes the application of the constant separation approach to the calculation of RUMs in three representative linearly bridged framework topologies: the Prussian Blue, $Zn(CN)_2$, and extended β-quartz families. The number and distribution of RUMs in the first two of these have been calculated previously elsewhere—but this has only been presented in terms of a simple counting of modes at different wave vectors.[30] The nature of these modes has not been systematically explored, nor have the effects of symmetry been considered. For these reasons their consideration here remains of interest because it serves to illustrate the level of information one can hope to determine through the constant separation approach. The extended β-quartz framework is also included here because—unlike the two other framework topologies considered—its structure necessarily contains linear bridges with nonideal geometries.

A. Prussian Blue structure type

The idealized Prussian Blue (PB) framework consists of a cubic array of octahedral coordination polyhedra, connected at each vertex by linear rods [Fig. 1(b)]. This family is a three-dimensional analog of the Simon and Varma system of connected squares. In real compounds of this type, one finds two primary variations on the idealized topology:[24,25,27] on the one hand, it is common for different types of metal center to be included in the framework, so that not all coordination octahedra are equivalent; on the other hand, a number of PB analogs—including PB itself—contain metal vacancies throughout the crystal lattice. The first of these aspects has no bearing on the topology of the framework, whereas the second introduces an additional level of flexibility that is dealt with separately below. The existence of RUMs in this broad family is of particular interest because its members have recently been reported to exhibit NTE behavior,[29,31,32] interesting sorption properties,[31] and the potential for gas storage applications.[43]

1. Vacancy-free frameworks

It is possible to characterize the family of vacancy-free Prussian Blues in terms of a framework with only one type of metal center. Examples of ideal PBs of this sort are $Fe[Fe(CN)_6]$ (Prussian Brown/Prussian Yellow),[44,45] $Ga(CN)_3$ (Refs. 28 and 46), and $Al(CN)_3$ (Ref. 47). The framework unit cell has $Pm\bar{3}m$ symmetry and contains just one polyhedron: an octahedron centered at position 1*a* with vertices at positions 6*e*. The constant separation interactions

TABLE I. RUMs in the defect-free Prussian Blue and $Zn(CN)_2$ frameworks. Zone-center acoustic modes are given in parentheses.

Wave vector	Prussian Blues	$Zn(CN)_2$
$\langle 0\ 0\ 0\rangle^*$	$3\Gamma_9$ $(+3\Gamma_{10})$	$3\Gamma_8+3\Gamma_9$ $(+3\Gamma_{10})$
$\langle 0\ 0\ \frac{1}{2}\rangle^*$	$X_2+2X_5+2X_6$	$2X_1+2X_3+4X_4$
$\langle 0\ \frac{1}{2}\ \frac{1}{2}\rangle^*$	$2M_5+M_7+M_8$	$2M_1+4M_2+2M_3$
$\langle \frac{1}{2}\ \frac{1}{2}\ \frac{1}{2}\rangle^*$	$3R_8$	$3R_7+3R_8+3R_9$
$\langle 0\ 0\ \xi\rangle^*$	$\Delta_2+4\Delta_3$	$\Delta_2+6\Delta_3+\Delta_4$
$\langle 0\ \xi\ \xi\rangle^*$	$\Sigma_2+\Sigma_3+2\Sigma_4$	$\Sigma_1+2\Sigma_2+3\Sigma_3+2\Sigma_4$
$\langle \xi\ \xi\ \xi\rangle^*$	$\Lambda_2+2\Lambda_3$	$2\Lambda_2+6\Lambda_3$
$\langle \frac{1}{2}\ \xi\ \xi\rangle^*$	$S_1+S_2+S_3$	$S_1+2S_2+3S_3+2S_4$
$\langle \frac{1}{2}\ \frac{1}{2}\ \xi\rangle^*$	$2T_3+T_4$	$6T_1+T_3+T_4$
$\langle \xi\ \zeta\ \eta\rangle^*$	3	8

occur between octahedra in adjacent unit cells; e.g., between the $(0,0,x)$ vertex of the octahedron in cell (0,0,0) and the $(0,0,-x)$ vertex of that in cell (0,0,1). Many of the terms in Eq. (4) vanish, to give the dynamical matrix

$$\mathbf{D}(\mathbf{k}) = 2K\left[\begin{array}{ccc|c} 1-\cos 2\pi\xi & 0 & 0 & \\ 0 & 1-\cos 2\pi\zeta & 0 & \star \\ 0 & 0 & 1-\cos 2\pi\eta & \\ \hline & \star & & \star \end{array}\right],$$

where ξ,ζ,η are the reduced components of $\mathbf{k}$ parallel to $\mathbf{a}^*$, $\mathbf{b}^*$, $\mathbf{c}^*$, and "$\star$" represents a 3×3 null submatrix.[37]

The symmetry-reduced forms of the dynamical matrix give the RUM labelings listed in Table I. However, it is also worthwhile considering general properties of the (nonreduced) matrix at arbitrary wave vector. This is only possible here because the matrix is sufficiently simple to treat analytically. Most noticeably, three of the eigenvalues (given by the last three diagonal entries) are zero irrespective of the particular value of $\mathbf{k}$. The associated eigenvectors correspond to displacements along each of $\theta_x,\theta_y,\theta_z$, and so represent rotations of the octahedra about the three Cartesian axes. These are the three rotational RUMs that decouple of the rotational degrees of freedom of each octahedron in the lattice: any given pattern of octahedral rotations can be viewed as a linear superposition of these RUMs at appropriate wave vectors.

The three remaining eigenvalues—namely $2K(1-\cos 2\pi\xi)$, $2K(1-\cos 2\pi\zeta)$, and $2K(1-\cos 2\pi\eta)$—correspond to translational displacements and are equal to zero if and only if $\xi=0$, $\zeta=0$, or $\eta=0$, respectively. Clearly at $\mathbf{k}=0$ these are the lattice translations, but this analysis also predicts the existence of two degenerate translational soft modes along X (the $2X_5$ modes), and one soft mode across the reciprocal lattice planes $\langle\xi\zeta 0\rangle^*$. The displacement patterns associated with each of these types of soft acoustic mode are illustrated in Fig. 3. The X_5 modes involve translations of planes of connected octahedra along any direction parallel to the plane itself: these sheets have two translational degrees of freedom. Similarly, the RUMs across $\langle\xi\zeta 0\rangle^*$ describe translations of individual columns of connected octahedra along a direction parallel to the column axis: each such column retains one of its translational degrees of freedom. While these RUMs may prove important in the physical properties of such frameworks, their density in reciprocal space—$O(V^{2/3})$ and $O(V^{1/3})$, respectively—is significantly less than that of the rotational RUMs. Consequently their relative involvement in bulk thermodynamic quantities such as thermal expansion behavior may prove limited.

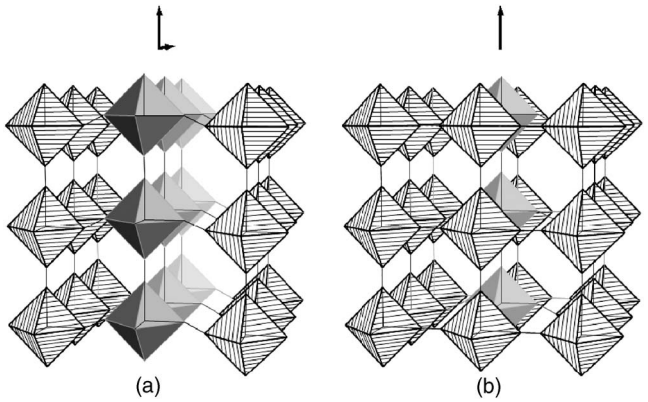

FIG. 3. Examples of localized translational RUMs in the idealized Prussian Blue topology at wave vectors (a) $\mathbf{k}\in X$ and (b) $\mathbf{k}\in\langle\xi\zeta 0\rangle^*$. In (a) sheets of connected octahedra translate along a direction parallel to the plane itself; in (b) columns of octahedra translate along a direction parallel to the column axis.

2. Partially vacant Prussian Blues

The incorporation of vacancies into the PB (or indeed any) framework topology can only be expected to increase structural flexibility, as doing so reduces the number of constraints on those rigid units adjoining the vacant site. Access to an automated method of computing RUMs in linearly bridged frameworks offers a robust mechanism of quantifying this increase in flexibility for PB-type materials. A number of important members of this family contain vacancies: PB itself,[48] the related compound Berlin Green,[44,45,49] high T_c molecular magnets such as $V^{II}[Cr^{III}(CN)_6]_{0.86}\cdot 2.8H_2O$ (Ref. 50), and gas storage candidates such as $Mn^{II}_3[Co^{III}(CN)_6]_2$ (Refs. 35 and 43).

The precise nature of vacancy inclusion can be very difficult to ascertain, and in general a semirandom distribution with $Fm\bar{3}m$ symmetry is assumed.[27] In this picture, the nondeficient cation occupies the $4a$ sites with an occupancy of 1, while the vacancies are distributed randomly across the $4b$ sites. Reflections forbidden in this space group were observed in a very careful single crystal study of PB by Buser *et al.*, indicating that under certain conditions there is evidence of vacancy ordering.[48] These additional reflections could be accounted for by a $Pm\bar{3}m$ structure in which the nondeficient cation occupies the $1a$ and $3c$ sites (equivalent to the $4a$ sites in $Fm\bar{3}m$) with an occupancy of 1, and the vacancies are distributed over the $1b$ and $3d$ sites. The authors reported that approximately 75% of the vacant sites were found at the $1b$ position with the remainder randomly distributed over the $3d$ sites.

These two vacancy distribution models were investigated using the LUSH program with the objective of ascertaining the effect of vacancy inclusion on framework flexibility in both regimes. In each case, the calculations were performed using a $4\times4\times4$ supercell of the vacancy-free unit cell, with an appropriate number and distribution of vacant sites. The supercells were constructed with effective compositions $M_A[M_B(\mathrm{CN})_6]_{1-x}\square_x\cdot y\mathrm{H_2O}$, $0\leqslant x<0.688$.[51] In this representation, the M_A atoms lie at the center of the "nondeficient" coordination polyhedra discussed above, and so occupy the $1a$ and $3c$ sites in the lattice; conversely, the M_B atoms are present in substoichiometric quantities and their coordination polyhedra share with the vacancies $\square$ the $1b$ and $3d$ lattice sites.

Remarkably, irrespective of the particular number and distribution of vacant sites, each framework was found to possess precisely the same number of RUMs at arbitrary wave vector as the vacancy-free framework. Consequently, the number of RUMs *per rigid unit* increases systematically as the vacancy concentration increases—this relative density is the most important measurable quantity as it determines the spectral weight of the RUMs. It is easily shown that the average number of degrees of freedom per rigid unit in these partially vacant PB analogs is given by

$$A=\frac{6}{2-x}. \tag{5}$$

At first sight, it is perhaps counterintuitive that the number of RUMs should be unaffected by the removal of polyhedra from the PB framework: the rotational independence of each polyhedron accounts for three RUMs, and these will vanish with the polyhedron itself. However, each vacant site necessarily lies at the intersection of three independent "columns" of octahedra, each of which will encounter further vacancies at some point in the lattice. That portion of the column that lies between pairs of vacancies will be free to translate parallel to the column axis. This type of translational freedom—along each of the three independent column systems—accounts for the three "lost" rotational RUMs. Moreover, its nature explains the increasingly translational character of the RUMs at arbitrary wave vector as the value of x increases. Indeed at $x=\frac{1}{2}$, Eq. (5) gives that $A=4$; that is, on average, each rigid unit is not only free to rotate but its motion along one direction is completely unconstrained.

The absolute number of RUMs along X and across the $\langle\xi\zeta0\rangle^*$ planes does, however, decrease as x increases: the translational RUM density becomes delocalized from these sets of wave vectors with its increasing contribution to the RUMs at arbitrary wave vector. The relative rate of decrease differed consistently between the two vacancy ordering models, such that the $Fm\bar{3}m$ distribution pattern showed a stronger dependency than the $Pm\bar{3}m$ variant. It is possible that this difference might provide a means of comparing distribution patterns through analysis of diffuse scattering intensities and their variation with vacancy composition.

B. $Zn(CN)_2$ structure type

The crystal structure of the $Zn(CN)_2$ family of compounds is related to that of β-cristobalite in the same way that the Prussian Blue and perovskite topologies might be compared: $[Zn(C/N)_4]$ coordination tetrahedra are connected via linear CN bridges to give an anticuprite lattice with cubic symmetry [Fig. 4(a)].[28,52] The tetrahedra are sufficiently well spaced that room is available for a second identical network to interpenetrate the first. These two networks are related by an inversion center and so raise the symmetry of the lattice from the $Fd\bar{3}m$ β-cristobalite unit cell to a $Pn\bar{3}m$ unit cell of one-eighth the volume. The orientation of the cyanide ions is disordered in this structure,[28] so that the unit cell contains two Zn atoms on the $2a$ sites and eight C/N atoms on the $8e$ positions.

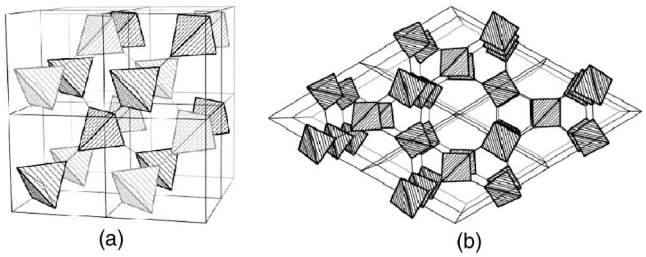

FIG. 4. Polyhedral representations of the (a) $Zn(CN)_2$ and (b) extended β-quartz framework topologies. The two interpenetrating lattices in (a) have been shaded differently. The quartz framework in (b) is a single connected lattice, and is viewed slightly away from the **c** crystal axis.

This family has emerged as perhaps one of the most important collections of NTE compounds: its members exhibit the strongest isotropic NTE effect yet reported.[28,30,31] Moreover, it is known that the structure type supports RUMs at all points in reciprocal space,[30] although their precise nature is not well-understood. It seems clear that the RUMs play an important—if not definitive—role in the observed NTE behavior since each acts to contract the lattice. It is possible that RUMs are also responsible for a low temperature phase transition reported in $Cd(CN)_2$ (Ref. 30).

The RUMs were calculated using the LUSH code, and the corresponding symmetry labelings are listed in Table I. The form of the (nonreduced) dynamical matrix is somewhat more complex in this case than for the idealized Prussian Blue topology:

$$\mathbf{D}(\mathbf{k})=\frac{4}{3}K\left[\begin{array}{ccc|c|ccc|c}
-1 & 0 & 0 & & x_1 & x_2 & x_3 & \\
0 & -1 & 0 & \star & x_2 & x_1 & x_4 & \star \\
0 & 0 & -1 & & x_3 & x_4 & x_1 & \\
\hline
 & \star & & \star & & \star & & \star \\
\hline
x_1^* & x_2^* & x_3^* & & -1 & 0 & 0 & \\
x_2^* & x_1^* & x_4^* & \star & 0 & -1 & 0 & \star \\
x_3^* & x_4^* & x_1^* & & 0 & 0 & -1 & \\
\hline
 & \star & & \star & & \star & & \star
\end{array}\right], \tag{6}$$

where

$$x_1=-\cos\pi\xi\cos\pi\zeta\cos\pi\eta+i\sin\pi\xi\sin\pi\zeta\sin\pi\eta,$$

$$x_2=+\sin\pi\xi\sin\pi\zeta\cos\pi\eta-i\cos\pi\xi\cos\pi\zeta\sin\pi\eta,$$

$$x_3 = +\sin \pi\xi \cos \pi\zeta \sin \pi\eta - i \cos \pi\xi \sin \pi\zeta \cos \pi\eta,$$

$$x_4 = +\cos \pi\xi \sin \pi\zeta \sin \pi\eta - i \sin \pi\xi \cos \pi\zeta \cos \pi\eta.$$

Despite this increased complexity, it is again apparent that some general properties of this matrix can be deduced. For example, 6 of the 12 eigenvalues are zero irrespective of the value of the wave vector; the corresponding eigenvectors describe rotations of the rigid units about the three Cartesian axes. As a consequence, arbitrary rotations of the $[Zn(C/N)_4]$ coordination polyhedra can always be accommodated through linear superpositions of RUMs. It can also be shown that the translational submatrix

$$\mathbf{D}_{\text{trans}}(\mathbf{k}) = \frac{4}{3}K \left[\begin{array}{ccc|ccc} -1 & 0 & 0 & x_1 & x_2 & x_3 \\ 0 & -1 & 0 & x_2 & x_1 & x_4 \\ 0 & 0 & -1 & x_3 & x_4 & x_1 \\ \hline x_1^* & x_2^* & x_3^* & -1 & 0 & 0 \\ x_2^* & x_1^* & x_4^* & 0 & -1 & 0 \\ x_3^* & x_4^* & x_1^* & 0 & 0 & -1 \end{array}\right]$$

is a rank four matrix for all wave vectors except $\mathbf{k}=\langle 000\rangle^*$, $\langle \frac{1}{2}\frac{1}{2}\frac{1}{2}\rangle^*$ (for which values it has a rank of three); consequently, there are two additional RUMs at arbitrary wave vector—both of purely translational character. At the zone center and the zone corners there is a third zero-frequency mode, such that the three translational RUMs correspond to translations of the entire lattice (the $3\Gamma_{10}$ modes) or the two interpenetrating networks in opposite directions (the $3R_7$ modes).

Just as the presence of rotational RUMs at arbitrary wave vector signals the rotational independence of polyhedra in this lattice, so too does the density of translational RUMs across reciprocal space imply some degree of translational freedom. There must exist some mechanism of translating individual polyhedra or isolated groups of polyhedra without disturbing the surrounding lattice. To understand this mechanism in the $Zn(CN)_2$ framework, it is illustrative to consider first the analogous two-dimensional framework of linearly bridged triangles [Fig. 5(a)]. It can be shown that this structure possesses two rotational RUMs and one translational RUM at arbitrary wave vector; this implies one rotational degree of freedom (i.e., complete rotational independence) and 0.5 translational degrees of freedom per rigid unit. Like the $Zn(CN)_2$ framework, it is straightforward to visualize the mechanism of rotational freedom. The translational freedom arises through collective displacements of rings containing six connected triangles [Fig. 5(a)]. As each ring can move in only one way, the number of degrees of freedom this motion imparts is equal to $\frac{1}{6}$ per rigid triangle; however, each triangle is a member of three such rings, and so this motion accounts for all of the observed translational degrees of freedom.

A similar mechanism can be seen to operate in the $Zn(CN)_2$ lattice: in this case the collective motion involves six-membered cyclohexyl-like rings of connected tetrahedra [Fig. 5(b)]. Each rigid unit belongs to six independent rings of this sort; consequently these ring translations impart one translational degree of freedom per rigid unit—two degrees per unit cell. The RUM eigenvectors for a particular wave vector describe superpositions of these localized modes, correlated throughout the lattice with the appropriate periodicity.

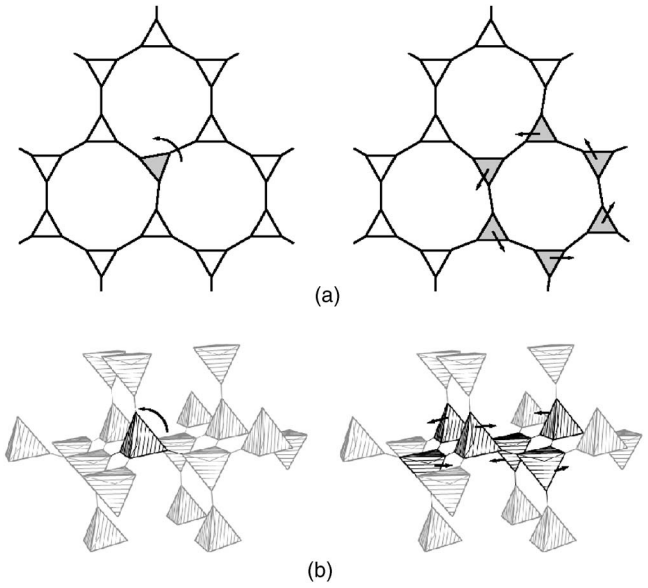

FIG. 5. Localized rigid-unit motion in the (a) two-dimensional linearly bridged "cristobalite" and (b) $Zn(CN)_2$ lattices. The left-hand panels illustrate the rotation of individual rigid units; the right-hand panels illustrate the correlated translation of rings of six rigid units.

C. Extended β-quartz structure type

Both the PB and $Zn(CN)_2$ topologies contain linearly bridged coordination polyhedra in ideal geometries: all equilibrium metal-linkage-metal angles are equal to 180°. The extended β-quartz framework contrasts these examples in the sense that it contains nonideal metal-linkage geometries: its average metal—linkage—metal angles deviate from 180° (but the distance constraints imposed by the linear linkages remain unaffected). There are only relatively few examples of compounds reported to exhibit this framework structure: $Zn[Au(CN)_2]_2$ (Refs. 53 and 54), $Zn[Ag(CN)_2]_2\cdot\{guest\}$ (Ref. 54), and $Co[Au(CN)_2]_2$ (Ref. 55). In each case, tetrahedrally coordinated metal centers are joined by pseudolinear dicyanometallate $[M(CN)_2]_2^-$ (M=Ag;Au) linkages to form a β-quartzlike network [Fig. 4(b)].[56] The networks contain large void regions that are occupied by the interpenetration of six identical nets to give crystal structures in either one of the enantiomorphic space groups $P6_222$ or $P6_422$. It appears that framework flexibility has a rather striking effect on various physical properties of these materials: both strongly isotropic NTE behavior and unusual host-guest properties have been observed in members of the family.[54]

In order to simplify the RUM analysis of this topology, it suffices to consider a single quartzlike framework: interpenetration has the sole effect of periodic repetition of the RUM spectrum at appropriate points in reciprocal space. Consequently it is possible to extrapolate from the RUM analysis

TABLE II. RUMs in the extended β-quartz framework. Zone-center acoustic modes are given in parentheses.

Wave vector	
$\langle 0\ 0\ 0\rangle^*$	$\Gamma_2+4\Gamma_3+2\Gamma_4+2\Gamma_5+\Gamma_6$ $(+\Gamma_2+2\Gamma_3)$
$\langle 0\ 0\ \frac{1}{2}\rangle^*$	$2A_1+6A_2+A_3+2A_5+A_6$
$\langle \frac{1}{2}\ 0\ 0\rangle^*$	$2M_1+5M_2+3M_3+2M_4$
$\langle \frac{1}{3}\ \frac{1}{3}\ 0\rangle^*$	$4K_2+8K_3$
$\langle \frac{1}{2}\ 0\ \frac{1}{2}\rangle^*$	$4L_1+3L_2+3L_3+2L_4$
$\langle \frac{1}{3}\ \frac{1}{3}\ \frac{1}{2}\rangle^*$	$8H_1+3H_2+H_3$
$\langle 0\ 0\ \xi\rangle^*$	$\Delta_1+3\Delta_2+\Delta_3+3\Delta_4+\Delta_5+3\Delta_6$
$\langle \frac{1}{2}\ 0\ \xi\rangle^*$	$7U_1+5U_2$
$\langle \xi\ 0\ 0\rangle^*$	$4\Sigma_1+8\Sigma_2$
$\langle \xi\ \xi\ 0\rangle^*$	$5\Lambda_1+7\Lambda_2$
$\langle \xi\ \xi\ \frac{1}{2}\rangle^*$	$5Q_1+7Q_2$
$\langle \xi\ \zeta\ \eta\rangle^*$	12

of a single framework to any number of interpenetrated frameworks. In the single-framework structure—which has a smaller unit cell but retains the original space group—the coordination polyhedra are centered on the $3c$ sites and the C/N atoms occupy nearby general positions. The RUMs were calculated using the LUSH code, and the results of this analysis are given in Table II.

In this case, there is little to be gained by consideration of the nonsymmetry-reduced dynamical matrix. The matrix is substantially more complex than that of either the PB or $Zn(CN)_2$ families; in particular, there are no longer any null submatrices. This allows mixing between rotational and translational degrees of freedom in the mode eigenvectors, and imposes a significant level of complexity to any attempted analysis. It is of interest nonetheless that the LUSH output reveals the presence of 12 RUMs at all wave vectors—with the exception of the zone center, where there exists an additional acoustic mode of zero frequency. Each tetrahedron in the lattice consequently possesses four degrees of freedom. From a counting perspective, this result mirrors the finding for $Zn(CN)_2$ frameworks; however, in this case the division between rotational and translational degrees of freedom is not so trivial. In particular, it is not possible to introduce arbitrary polyhedral rotations in the β-quartz lattice without inducing translations in connected rigid units. Localized flexibility in the β-quartz framework is similarly complex, but its existence is guaranteed by the observed density of RUMs at arbitrary wave vector, and may be responsible for the unusual host-guest properties observed in some of these materials.

IV. DISCUSSION AND CONCLUSIONS

At the most basic level, framework flexibility in connected polyhedral networks can be considered as a balance between the number of degrees of freedom F of each polyhedron and the number of constraints C placed on its position and orientation by the network connectivity. Indeed this approach has been used for some time in the glass community, where structural "floppiness" is predicted whenever $F > C$ (Refs. 57–62). A number of the "classical" frameworks (as defined in the Introduction) have provided a fascinating boundary condition of this methodology, for which $F=C$. For example, silicate frameworks such as quartz and cristobalite consist of connected tetrahedra with six degrees of freedom, and with six constraints (each connected vertex carries with it three positional constraints, shared by the two associated polyhedra). What RUM analysis has illustrated elegantly in these materials is that symmetry introduces a degree of redundancy into particular sets of constraints, and that some flexibility persists despite the apparent balance between F and C.

In contrast, connectivity in linearly bridged frameworks involves only one constraint for each pair of connected vertices: the distance by which they are separated. Moreover, this single constraint is shared between connected polyhedra, so that each linear linkage contributes only one-half of a constraint to the value of C. Linearly bridged frameworks with topologies analogous to tetrahedral silicates such as quartz and cristobalite will consequently possess only two constraints per coordination polyhedron. The excess $F-C=4$ degrees of freedom will be manifest in the accumulation of RUMs at arbitrary wave vector. This is precisely the situation observed for the $Zn(CN)_2$ and extended β-quartz topologies analyzed above: each was found to possess $4Z$ RUMs at arbitrary wave vector (Z being the number of rigid polyhedra per unit cell). In a similar manner, the idealized Prussian Blue structure contains octahedra with $F-C=3$ surplus degrees of freedom; these correspond to the three arbitrary-wave vector RUMs observed for this family.

The key result of this line of reasoning is that linearly bridged frameworks built from n-polyhedra are guaranteed at least $(6-n/2)Z$ RUMs at all points across the Brillouin zone. As such, the fraction of RUMs in the density of states χ_{RUM} will have the lower bound

$$\chi_{\mathrm{RUM}} \geqslant \frac{12-n}{6(n+1)}.$$

Some "classical" framework topologies—typically zeolites—are known to possess RUMs at all wave vectors despite the superficial condition $F=C$ (Refs. 19 and 20); consequently it is possible that some linearly bridged frameworks may carry more arbitrary wave vector RUMs than those inherent in the remnant $F-C$ degrees of freedom. It should be noted that the perovskite, cristobalite, and quartz frameworks (the "classical" analogs of the linearly bridged systems analyzed in Sec. III) possess RUMs only within specific regions of reciprocal space.[7]

For those frameworks with equilibrium metal-linkage angles of 180°, it is possible to draw some general conclusions about localized flexibility from the theoretical framework of Sec. II. In these systems, the normalized linkage vectors $\boldsymbol{\rho}$ are necessarily parallel to the associated vertex vectors $\mathbf{e}_j$. Consequently, Eq. (3) simplifies to give

$$\Delta d = -\boldsymbol{\rho}\cdot(\mathbf{u}_j - \mathbf{u}_{j'}).$$

For the same reason, all entries in the submatrices B, C, and D of Eq. (4) vanish under these conditions. The absence of

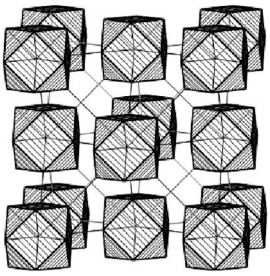

FIG. 6. Representation of a theoretical dodecahedrally coordinated linearly bridged framework structure. Despite the balance between the numbers of constraints and degrees of freedom in this topology, the framework possesses three rotational RUMs at arbitrary wave vector. This occurs because all metal-linkage geometries have equilibrium angles of 180°.

any rotational displacement terms means that the dynamical matrix contains empty rows and columns wherever these correspond to rotational degrees of freedom; the corresponding $3Z$ matrix eigenvalues will be identically zero, with the associated eigenvectors describing rotations of the Z rigid units about the Cartesian axes. Because these RUMs exist at arbitrary wave vector, it is an intrinsic property of such frameworks that the rigid coordination polyhedra have complete rotational independence. This result persists irrespective of the coordination number n: even the theoretical dodecahedral structure of Fig. 6 possesses these rotational RUMs despite the value $F-C=0$ implied by its 12-fold linear coordination.

What has emerged from this study is that localized flexibility is an intrinsic property of linearly bridged framework structures. A rigorous understanding of this flexibility has followed from the "constant separation" dynamical matrix approach, which has allowed topology-independent generalizations to be drawn. The implementation of this method in the program LUSH has been employed systematically to identify the RUMs in three important families and to label these according to the relevant crystal symmetries. Their large spectral weight has two primary ramifications for the physical properties of these materials. On the one hand, the RUMs can be expected to contribute substantially to thermodynamic properties such as thermal expansion behavior—and especially so because of their low energies. On the other hand, the associated flexibility allows low-energy local distortions of the sort required for sorption phenomena and catalytic behavior; but perhaps the most important result is that these properties can be expected to permeate all members of the diverse family of linearly bridged framework materials. The rich spectrum of properties attributed to RUMs in "classical" systems can only intensify and broaden in these fascinating compounds.

ACKNOWLEDGMENTS

The author thanks M. T. Dove for useful discussions, and Trinity College, Cambridge for financial support.

[1] A. F. Wells, *Structural Inorganic Chemistry* (Clarendon, Oxford, England, 1984).
[2] H. D. Megaw, *Crystal Structures: A Working Approach* (Saunders, Philadelphia, 1973).
[3] A. M. Glazer, Acta Crystallogr., Sect. B: Struct. Crystallogr. Cryst. Chem. **B28**, 3384 (1972).
[4] H. Boysen, B. Dorner, F. Frey, and H. Grimm, J. Phys. C **13**, 6127 (1980).
[5] B. Berge, J. P. Baccheimer, G. Dolino, M. Vallade, and C. M. E. Zeyen, Ferroelectrics **66**, 73 (1985).
[6] M. Vallade, B. Berge, and G. Dolino, J. Phys. I **2**, 1481 (1992).
[7] A. P. Giddy, M. T. Dove, G. S. Pawley, and V. Heine, Acta Crystallogr., Sect. A: Found. Crystallogr. **A49**, 697 (1993).
[8] A. K. A. Pryde, K. D. Hammonds, M. T. Dove, V. Heine, J. D. Gale, and M. C. Warren, J. Phys.: Condens. Matter **8**, 10973 (1996).
[9] J. Z. Tao and A. W. Sleight, J. Solid State Chem. **173**, 442 (2003).
[10] J. S. O. Evans, J. Chem. Soc. Dalton Trans. **1999**, 3317 (1999).
[11] G. D. Barrera, J. A. O. Bruno, T. H. K. Barron, and N. L. Allan, J. Phys.: Condens. Matter **17**, R217 (2005).
[12] M. G. Tucker, A. L. Goodwin, M. T. Dove, D. A. Keen, S. A. Wells, and J. S. O. Evans, Phys. Rev. Lett. **95**, 255501 (2005).
[13] P. B. Allen, Y.-R. Chen, S. Chaudhuri, and C. P. Grey, Phys. Rev. B **73**, 172102 (2006).
[14] K. Trachenko, cond-mat/0604617 (unpublished).
[15] K. Trachenko, M. T. Dove, V. Brazhkin, and F. S. El'kin, Phys. Rev. Lett. **93**, 135502 (2004).
[16] P. Boolchand, G. Lucovsky, J. C. Phillips, and M. F. Thorpe, Philos. Mag. **85**, 3823 (2005).
[17] J. C. Phillips, Phys. Rev. B **73**, 104206 (2006).
[18] M. F. Thorpe and M. Lei, Philos. Mag. **84**, 1323 (2004).
[19] K. D. Hammonds, H. Deng, V. Heine, and M. T. Dove, Phys. Rev. Lett. **78**, 3701 (1997).
[20] K. D. Hammonds, V. Heine, and M. T. Dove, J. Phys. Chem. B **102**, 1759 (1998).
[21] A. Sartbaeva, S. A. Wells, and S. A. T. Redfern, J. Phys.: Condens. Matter **16**, 8173 (2004).
[22] A. L. Goodwin, S. A. Wells, and M. T. Dove, Chem. Geol. **225**, 213 (2006).
[23] M. E. Simon and C. M. Varma, Phys. Rev. Lett. **86**, 1781 (2001).
[24] A. Ludi and H. U. Güdel, Struct. Bonding (Berlin) **14**, 1 (1973).
[25] A. G. Sharpe, *The Chemistry of Cyano Complexes of the Transition Metals* (Academic Press, London, England, 1976).
[26] K. R. Dunbar and R. A. Heintz, Prog. Inorg. Chem. **45**, 283 (1997).
[27] M. Verdaguer and G. Girolami, in *Magnetism: Molecules to Materials V*, edited by J. S. Miller and M. Drillon (Wiley-VCH Verlag GMbH & Co., Weinheim, 2004).
[28] D. Williams, D. E. Partin, F. J. Lincoln, J. Kouvetakis, and M. O'Keeffe, J. Solid State Chem. **134**, 164 (1997).
[29] S. Margadonna, K. Prassides, and A. N. Fitch, J. Am. Chem. Soc. **126**, 15390 (2004).
[30] A. L. Goodwin and C. J. Kepert, Phys. Rev. B **71**, 140301(R)

(2005).
[31] K. W. Chapman, P. J. Chupas, and C. J. Kepert, J. Am. Chem. Soc. **127**, 15630 (2005).
[32] A. L. Goodwin, K. W. Chapman, and C. J. Kepert, J. Am. Chem. Soc. **127**, 17980 (2005).
[33] T. Pretsch, K. W. Chapman, G. J. Halder, and C. J. Kepert, Chem. Commun. (Cambridge) **2006**, 1857 (2006).
[34] K. W. Chapman, P. J. Chupas, and C. J. Kepert, J. Am. Chem. Soc. **128**, 7009 (2006).
[35] K. W. Chapman, P. J. Chupas, and C. J. Kepert, J. Am. Chem. Soc. **127**, 11232 (2005).
[36] A. L. Goodwin, Ph.D. thesis, University of Sydney, 2003.
[37] Here, as elsewhere in the paper, unit masses and moments of inertia are assumed: this simplification affects only the scaling of the calculated mode frequencies, but not the number and nature of RUMs.
[38] A. A. Maradudin and S. H. Vosko, Rev. Mod. Phys. **40**, 1 (1968).
[39] J. L. Warren, Rev. Mod. Phys. **40**, 38 (1968).
[40] G. S. Pawley, Phys. Status Solidi B **49**, 475 (1972).
[41] J. L. Warren and T. G. Worlton, Comput. Phys. Commun. **8**, 71 (1974).
[42] T. G. Worlton and T. G. Warren, Comput. Phys. Commun. **3**, 88 (1972); **4**, 382 (1972).
[43] K. W. Chapman, P. D. Southon, C. L. Weeks, and C. J. Kepert, Chem. Commun. (Cambridge) **2005**, 3322 (2005).
[44] J. F. de Wet and R. Rolle, Z. Anorg. Allg. Chem. **336**, 96 (1965).
[45] K. Maer, Jr., M. L. Beasley, R. L. Collins, and W. O. Milligan, J. Am. Chem. Soc. **90**, 3201 (1968).
[46] L. C. Brousseau, D. Williams, J. Kouvetakis, and M. O'Keeffe, J. Am. Chem. Soc. **119**, 6292 (1997).
[47] D. Williams, B. Pleune, K. Leinenweber, and J. Kouvetakis, J. Solid State Chem. **159**, 244 (2001).
[48] H. J. Buser, D. Schwarzenbach, W. Petter, and A. Ludi, Inorg. Chem. **16**, 2704 (1977).
[49] A. Kumar, S. M. Yusuf, and L. Keller, Phys. Rev. B **71**, 054414 (2005).
[50] S. Ferlay, T. Mallah, R. Ouahès, P. Veillet, and M. Verdaguer, Nature (London) **378**, 701 (1995).
[51] In practice, the vast majority of PB analogs correspond to vacancy concentrations $0 \leqslant x \leqslant 0.333$; the upper limit chosen here corresponds to the percolation threshold required to maintain framework connectivity.
[52] B. F. Hoskins and R. Robson, J. Am. Chem. Soc. **112**, 1546 (1990).
[53] B. F. Hoskins, R. Robson, and N. Y. Scarlett, Angew. Chem., Int. Ed. Engl. **34**, 1203 (1995).
[54] A. L. Goodwin, B. J. Kennedy, and C. J. Kepert (unpublished).
[55] S. C. Abrahams, L. E. Zynotz, and J. L. Bernstein, J. Chem. Phys. **76**, 5458 (1982).
[56] The term "pseudo-linear" is used here to reflect the fact that in these structures the dicyanometallate anion linkages are slightly bent. In spite of this, they act topologically in an identical manner to "perfectly" linear linkages, in that they place only one constraint on the coordination polyhedra they connect: namely, the distance between the connected vertices. There will be some additional vibrational component due to internal modes of the dicyanometallate bridges; indeed, in practice it is likely that the distance constraint imposed by these extended linkages will be modestly weaker than that of individual C-N linkages. Nevertheless, the primary source of flexibility in these frameworks is through bending of the metal-cyanide linkages, and so to a first-order approximation the internal modes of the pseudo-linear linkages will not affect the RUM analysis.
[57] J. C. Phillips, J. Non-Cryst. Solids **34**, 153 (1979).
[58] J. C. Phillips, J. Non-Cryst. Solids **43**, 37 (1981).
[59] G. H. Döhler, R. Dandoloff, and H. Bilz, J. Non-Cryst. Solids **42**, 87 (1980).
[60] M. F. Thorpe, J. Non-Cryst. Solids **57**, 3355 (1983).
[61] H. He and M. F. Thorpe, Phys. Rev. Lett. **54**, 2107 (1985).
[62] Y. Cai and M. F. Thorpe, Phys. Rev. B **40**, 10535 (1989).